Flash spectroscopic studies of the kinetics of the halorhodopsin photocycle

ARTICLE *in* BIOCHEMISTRY · MARCH 1986

Impact Factor: 3.02 · DOI: 10.1021/bi00354a042 · Source: PubMed

2 AUTHORS, INCLUDING:

Vitaly Vodyanoy
Auburn University
227 PUBLICATIONS **2,012** CITATIONS

Flash Spectroscopic Studies of the Kinetics of the Halorhodopsin Photocycle†

Janos K. Lanyi* and Vitaly Vodyanoy

Department of Physiology and Biophysics, University of California, Irvine, California 92717

Received July 24, 1985

ABSTRACT: The photoreactions of halorhodopsin are complicated by the fact that the parent pigment and its photoproducts interact with chloride. Thus, in any photoreaction scheme at least four species have to be accounted for: HR_{565} and $HR_{578}{\cdot}Cl^-$, as well as HR_{640} and $HR_{520}{\cdot}Cl^-$. A photocycle scheme proposed earlier places the two main photointermediates of halorhodopsin, $HR_{520}{\cdot}Cl^-$ and hR_{640}, into a single photocycle, with a chloride-dependent equilibrium between them [Oesterhelt, D., Hegemann, P., & Tittor, J. (1985) *EMBO J. 4*, 2351–2356]. This scheme, with the additional feature of direct photoproduction of HR_{640} from HR_{565}, was tested in this work by using numerical solutions of the appropriate differential equations to simulate flash-induced absorption changes at 500 nm (production of $HR_{520}{\cdot}Cl^-$) and at 660 nm (production of HR_{640}). The time scale of the simulation was 20 ms following the flash. Comparison of the simulated curves with experimental traces yielded a unique set of three rate constants. The proposed photocycle scheme and these rate constants predict well the shapes and amplitudies of flash traces at various chloride concentrations. It appears from the photocycle scheme, and the numerical values of the rate constants, that chloride is bound with high affinity to the parent halorhodopsin molecule, but with much lower affinity to its main photointermediate. This may be the consequence of the fact that in the parent halorhodopsin the retinal configuration is all-trans, but in the two photointermediates it is 13-cis.

Halorhodopsin is a retinal protein similar to bacteriorhodopsin (Stoeckenius & Bogomolni, 1982; Lanyi, 1984a; 1986), but it functions as a light-driven chloride pump (Schobert & Lanyi, 1982; Bamberg et al., 1984), rather than a light-driven proton pump. Like the other pigment, halorhodopsin undergoes a cyclic reaction upon illumination, and it yields two transient photoproducts on a millisecond time scale, labeled HR_{520}[1] and HR_{640} (Stoeckenius & Bogomolni, 1982; Tsuda et al., 1982; Schobert et al., 1983). The yield of these photointermediates is dependent on the presence of chloride and its concentration (Schobert et al., 1983). Some proposed schemes (Stoeckenius & Bogomolni, 1982; Schobert et al., 1983) related this chloride dependency to the fact that under some conditions chloride causes a red shift in the absorption spectrum of halorhodopsin (Ogurusu et al., 1982; Steiner et al., 1984; Schobert et al., 1985), consistent with the existence of two species of halorhodopsin, HR_{565} (in the absence of chloride) and $HR_{578}{\cdot}Cl^-$ (in the presence of chloride). Thus, HR_{565} was suggested to yield HR_{640} upon illumination and $HR_{578}{\cdot}Cl^-$ to yield $HR_{520}{\cdot}Cl^-$ (Stoeckenius & Bogomolni, 1982). A modification of this kind of scheme was made when it became apparent that the decay kinetics of both $HR_{520}{\cdot}Cl^-$ and HR_{640} were dependent on the chloride concentration (Schobert et al., 1983), and chloride-dependent equilibria were suggested for each of these intermediates also. None of the photocycle schemes include an intermediate with a deprotonated Schiff base.

It has become apparent since these schemes were suggested that there are two kinds of anion binding sites in halorhodopsin which produce changes detectable by spectroscopic means. The first of these, site I, is rather nonspecific and has a direct influence on the retinal Schiff base because its occupancy results in an increase in the pK_a of Schiff-base deprotonation (Lanyi & Schobert, 1983; Steiner et al., 1984; Schobert et al., 1986). Binding of an anion exclusively to site I (e.g., in equilibrium experiments with nitrate or thiocyanate) causes a small blue shift in the chromophore spectrum, and produces HR_{565} (Schobert et al., 1986). The second site, site II, is restricted to chloride and bromide (and iodide), and its occupation produces a small red shift in the presence of nonhalide site I anions (Ogurusu et al., 1982; Schobert et al., 1985), yielding $HR_{578}{\cdot}Cl^-$. The photointermediate $HR_{520}{\cdot}Cl^-$ is produced in detectable quantities only when site II is occupied. The specificity of site II agrees with the specificity of transport by halorhodopsin (Schobert & Lanyi, 1982; Bamberg et al., 1984; Hazemoto et al., 1984).

A different kind of photocycling scheme, suggested on the basis of the development of the spectra of the photointermediates at submillisecond intervals and the pathways of azide-catalyzed retinal Schiff-base deprotonation (Hegemann, 1984; Oesterhelt et al., 1985; Hegemann et al., 1985), puts $HR_{520}{\cdot}Cl^-$ and HR_{640} into a single photocycle, with a chloride-dependent interconversion step between these photointermediates. In this report we attempt to test a scheme that incorporates this feature by comparing traces of flash-induced absorption changes with simulated traces based upon the differential equations in the proposed model. The results confirm the validity of the scheme.

Materials and Methods

Halobacterium halobium strain OD-2 was grown in a peptone medium, as described before (Lanyi & MacDonald, 1979). Halorhodopsin was prepared by the Lubrol PX method (Steiner & Oesterhelt, 1983) but without the final exchange

† This work was supported by a grant from the National Aeronautics and Space Administration (NAGW-212).

[1] Abbreviations: MES, 2-(*N*-morpholino)ethanesulfonic acid. The halorhodopsin species are designated as follows: HR_{565}, parent species with site II unoccupied; $HR_{578}{\cdot}Cl^-$, parent species with site II occupied; HR_{640} and HR_x, photointermediates with site II unoccupied; $HR_{520}{\cdot}Cl^-$ and $HR_{600}{\cdot}Cl^-$, photointermediates with site II occupied. Site I is assumed to be occupied (by chloride, nitrate, or thiocyanate) under all conditions in this paper. This designation is followed also in citing other authors, even when their own notation is different.

0006-2960/86/0425-1465$01.50/0

of this detergent for octyl glucoside. The halorhodopsin samples were stored in 2 M NaCl, 20 mM MES, pH 6.0, and 1% Lubrol PX at 4 °C in the dark and were stable for months. For some experiments the samples were dialyzed against another buffer, as indicated. This was done just before the experiments, against two changes of 100 volumes, 2 h each at 4 °C in the dark.

Stationary spectra were obtained with a Gilford Model 2600 single-beam spectrophotometer. Flash-induced absorption changes were determined in a cross-beam flash spectrometer described before (Schobert et al., 1983), but the photomultiplier in some of the experiments was replaced with a photodiode (United Detector Technology, Model UDT-555UV), and the instrument was operated in the split-beam mode with a second detector (photodiode) for increased stability. As before (Lanyi & Schobert, 1983; Schobert et al., 1983), flash illumination was with a Photochemical Research Associates Model 610B pulsed light source, through either a red filter (when the measuring beam was at 500 nm), a combination of green filters (when the measuring beam was at 660 nm), or a yellow filter (when the measuring beam was in the near-UV). The effective intensities of these flashes were estimated by their ability to produce absorption change at 500 nm. The relative intensities of the red and green flashes were 1.25:1. Measurements in the near-UV were also as before (Lanyi, 1984b). Usually, signal averaging was for 512 repetitions.

Numerical solutions of the differential rate equations were obtained with an XPC computer equipped with a high-resolution graphics card, using spreadsheet software. The solutions simulated the time-dependent concentration of the photointermediates (i.e., absorption changes at 500 and 660 nm) during the first 20 ms after the flash. The time resolution of the solutions was 0.1 ms. The rate constants were fitted by visual comparison of the simulated traces with the experimental traces, as described under Results.

RESULTS

Flash-induced absorption changes were measured for halorhodopsin at 580 nm (depletion of the parent chromophore), at 500 nm (production of $HR_{520}{\cdot}Cl^-$), and at 660 nm (production of HR_{640}), as shown in Figure 1. All experiments were carried out both in 0.5 M Na_2SO_4 buffer containing 100 mM NaSCN and in 4 M NaCl buffer. The former buffer was intended for following the photoreaction of HR_{565}, the only species that exist under these conditions, with the thiocyanate added as a site I anion which confers increased stability (Steiner et al., 1984; Schobert et al., 1986). The latter buffer was for following the photoreaction of $HR_{578}{\cdot}Cl^-$, the major species present under these conditions. The results in Figure 1 show that, as reported before (Stoeckenius & Bogomolni, 1982; Schobert et al., 1983; Steiner et al., 1984), HR_{565} produces only HR_{640} in detectable amounts (trace E). At 500 nm nothing but the depletion of the parent chromophore is seen in this case (trace G), whose amplitude relative to the depletion at 580 nm (trace F) is consistent with the absorbance of halorhodopsin at these wavelengths. In contrast, $HR_{578}{\cdot}Cl^-$ gives rise to both $HR_{520}{\cdot}Cl^-$ (trace C) and HR_{640} (trace A), although the latter in a rather small amount. The photointermediate $HR_{520}{\cdot}Cl^-$ rises rapidly and decays slowly (trace C), similarly to the depletion trace in the chloride buffer (trace B). The shape of the HR_{640} traces is dependent on the salt used: this photointermediate rises rapidly and decays rapidly in sulfate buffer (trace E) but rises slowly and decays slowly in chloride buffer (trace A). Again, the depletion trace (trace F) reflects the behavior of the photointermediate produced in

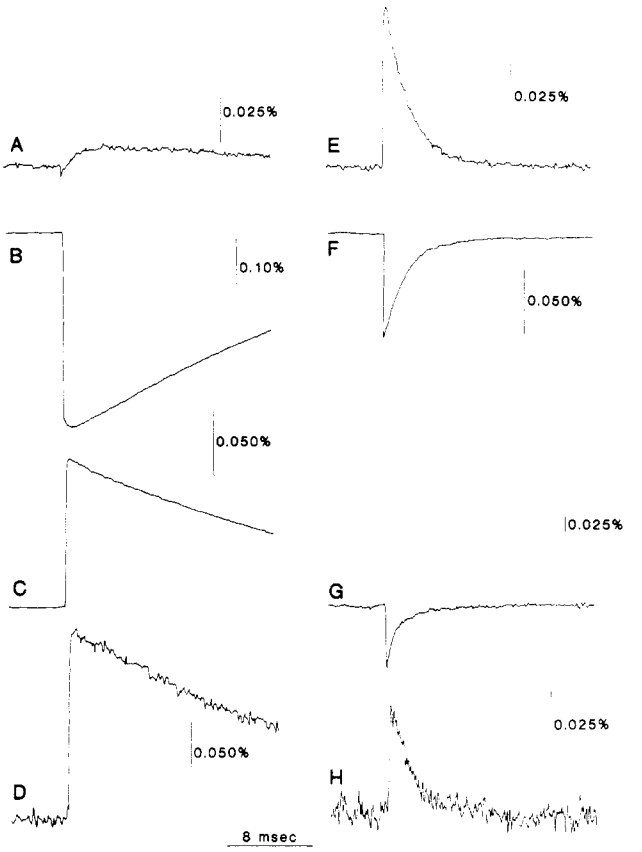

FIGURE 1: Flash-induced absorption changes obtained with halorhodopsin in different buffers and at different wavelengths. The halorhodopsin (4.4 nmol/mL) was in either 4.0 M NaCl and 20 mM MES, pH 6.0 (traces A–D), or 0.5 M Na_2SO_4, 100 mM NaSCN, and 10 mM phosphate, pH 6.0 (traces E–H). Wavelengths of the measurements: traces A and E, 660 nm; traces B and F, 580 nm; traces C and G, 500 nm; traces D and H, 340 nm. Vertical bars and their scales refer to the percent change in transmittance per flash. Time constant of the recording, 0.1 ms.

the sulfate. Calculations from the amplitudes of the two depletion traces (traces B and F) and the respective differential extinction coefficients indicated that the yield for HR_{640} is considerably less than the yield for $HR_{520}{\cdot}Cl^-$ (relative yields 0.36:1). The reduced quantum yield of the production of HR_{640} is not accounted for by the small blue shift of the absorption of its parent species and the resulting somewhat decreased overlapping with the spectrum of the flash. On the other hand, the difference in the quantum yields for the two conditions in Figure 1 is partly due to a small but distinct increase in the photoproduction yield for $HR_{520}{\cdot}Cl^-$ with NaCl concentration above 1 M, caused perhaps by salt-induced conformational changes in the pigment. At NaCl concentrations below 0.5 M, where most of the measurements in this report were carried out, the flash-induced difference spectra were consistent with a relative quantum yield of 0.6.

Traces D and H show measurements at 340 nm in chloride and sulfate buffers, respectively. It is evident that absorption changes at this wavelength occur not only in the chloride buffer as shown in an earlier report (Lanyi, 1984b) but also in the sulfate buffer. The kinetics of the decay in each buffer agrees well with the kinetics of decay of the main photointermediate in that buffer (compare traces C and D and traces E and H).

We have reported earlier (Lanyi, 1984b) that the flash-induced difference spectrum of halorhodopsin in the near-UV was dominated by the characteristic "cis peak" of retinal isomerization, and the changes seen in bacteriorhodopsin that originate from the deprotonation of a tyrosine (Hess &

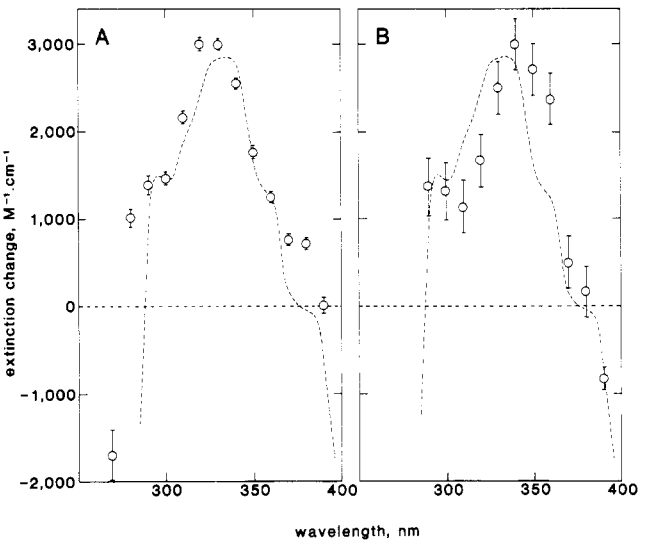

FIGURE 2: Flash-induced difference spectrum in the near-UV in different buffers. The experiments were as described in Figure 1; for (A) the buffer was 2.0 M NaCl and 20 mM MES, pH 6.0; for (B) the buffer was 0.5 M Na_2SO_4 plus 100 mM NaSCN and 10 mM phosphate, pH 6.0. The flash-induced changes in the extinction at each wavelength were calculated from the maximum absorption change immediately after the flash (see traces in Figure 1) and the amount of pigment photocycling, as explained in the text. The dashed lines are difference spectra for dark-adapted vs. light-adapted bacteriorhodopsin [redrawn from Lanyi (1984b)], on a scale that indicates the absorption changes expected for 100% isomerization.

Kuschmitz, 1979) are not present. It was concluded from this (Lanyi, 1984b) that the retinal configuration in $HR_{520}{\cdot}Cl^-$ is cis (perhaps 13-cis as in the photointermediates of bacteriorhodopsin), rather than all-trans as in the parent molecule (Smith et al., 1984; Alshuth et al., 1985; Maeda et al., 1985). Extraction and analysis of the retinal has demonstrated the 13-cis isomeric form in illuminated halorhodopsin when the pigment was trapped in a stable form during the illumination, either as the deprotonated product (Ogurusu et al, 1981) or as the oxime.[2] Flash-induced difference spectra, based on experiments similar to those in Figure 1, are shown in Figure 2. The absorption changes are given as extinction changes, calculated from the magnitudes of the flash-induced absorption changes at the indicated wavelengths and the amount of pigment that photocycled. The latter was estimated from the flash-induced bleaching at 580 nm by using differential extinction coefficients of 42 500 $M^{-1}{\cdot}cm^{-1}$ or 33 700 $M^{-1}{\cdot}cm^{-1}$ when the main photointermediates were $HR_{520}{\cdot}Cl^-$ or HR_{640}, respectively. Also included in Figure 2 is a difference spectrum of dark-adapted vs. light-adapted bacteriorhodopsin, redrawn from Figure 3B in Lanyi (1984b), which is the expected difference spectrum for 100% isomerization of the retinal in the photointermedates if it is assumed that only the isomerization (around the C_{13}/C_{14} double bond in bacteriorhodopsin) contributes to the changes (Hess & Kuschmitz, 1979). Roughly similar difference spectra to these were obtained for halorhodopsin in chloride (Figure 2A) and sulfate (Figure 2B) buffers, although, like the absorption bands in the visible, the absorption maxima in the near-UV are somewhat blue-shifted for $HR_{520}{\cdot}Cl^-$ and somewhat red-shifted for HR_{640}. We conclude that all-trans → cis isomerization occurs for both $HR_{520}{\cdot}Cl^-$ and HR_{640}. It seems likely that the isomerization produces the 13-cis isomer of retinal as in bacteriorhodopsin, but the difference spectra in Figure 2 would be consistent with

[2] P. Hegemann and D. Oesterhelt, unpublished experiments.

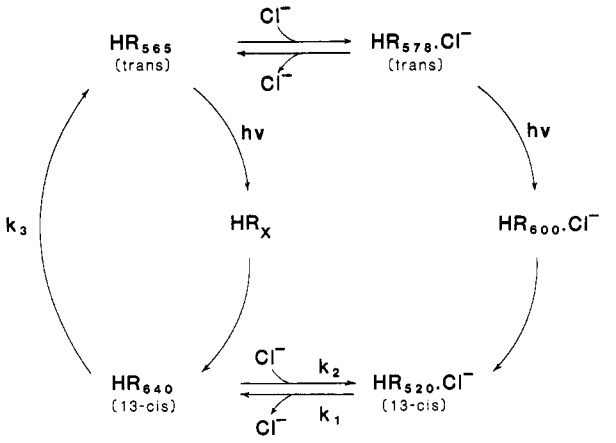

FIGURE 3: Suggested photocycle scheme for halorhodopsin. This scheme is essentially as proposed elsewhere (Hegemann, 1984; Hegemann et al., 1985; Oesterhelt et al., 1985), except that the isomeric state of the retinal is noted for some of the species, and a pathway for the photoconversion of HR_{565} to HR_{640} via HR_x is added.

other cis isomers as well. The magnitude of the change is consistent with essentially 100% of the photocycling fraction isomerizing.

As shown in Figure 1, flash illumination of halorhodopsin under different conditions will produce a set of traces with characteristic amplitudes and shapes. We attempted to simulate these traces with a photocycle scheme suggested elsewhere from evidence not including flash spectroscopy (Hegemann, 1984; Hegemann et al., 1985; Oesterhelt et al., 1985). This suggested scheme is shown in Figure 3, with the additional feature of photoconversion of HR_{565} into HR_{640} via a so far undetected intermediate, HR_x, so that HR_{640} arises via two pathways: from HR_x directly and from $HR_{520}{\cdot}Cl^-$ by a chloride-dependent equilibrium. It is thus assumed in the scheme that the HR_{640} which arises from $HR_{520}{\cdot}Cl^-$ is the same HR_{640} which arises from HR_{565}. Direct evidence for this is not available at this time. All reactions not labeled with a rate constant were considered to be so rapid that they could be regarded as instantaneous at the time resolution available to us (cf. rise kinetics in Figure 1, traces B–H). The differential equations that describe the change in the concentrations of photointermediates are

$$d(HR_{520}{\cdot}Cl^-)/dt = k_2(HR_{640})(Cl^-) - k_1(HR_{520}{\cdot}Cl^-) \quad (1)$$

$$d(HR_{640})/dt = k_1(HR_{520}{\cdot}Cl^-) - k_2(HR_{640})(Cl^-) - k_3\,(HR_{640}) \quad (2)$$

Since the absolute quantum yield of the photoreactions is not of interest here, the maximum initial value of $(HR_{520}{\cdot}Cl^-)$ immediately after the flash was set at 1. Thus, the flash illumination enters into these calculations merely to set the initial concentrations of $HR_{520}{\cdot}Cl^-$ and HR_{640}, and the use of the usual photochemical equations is avoided. At chloride concentrations at which significant amounts of HR_{565} are present, the initial concentrations of the two photointermediates are given by the relationships:

$$(HR_{520}{\cdot}Cl^-)_{t=0} = \frac{1}{1 + K_D^{II}/(Cl^-)} \quad (3)$$

$$(HR_{640})_{t=0} = \frac{0.6}{1 + (Cl^-)/K_D^{II}} \quad (4)$$

where K_D^{II} is the dissociation constant that describes the equilibrium between HR_{565} and $HR_{578}{\cdot}Cl^-$ (i.e., binding of Cl^- to site II). K_D^{II} was earlier reported to be 10 mM (Steiner et al., 1984; Bamberg et al., 1984; Hazemoto et al., 1984) or

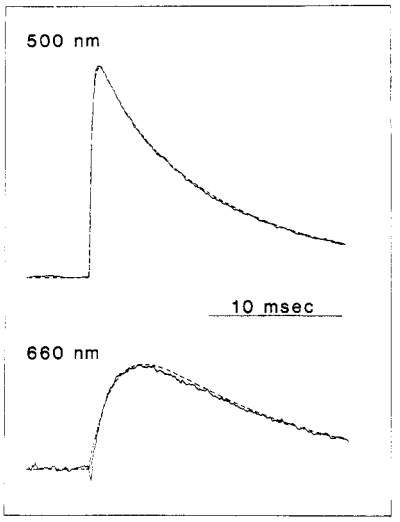

FIGURE 4: Flash-induced absorption change for halorhodopsin at 500 nm and at 660 nm. The halorhodopsin (7.2 nmol/mL) was in 0.5 M Na_2SO_4 plus 0.35 M NaCl and 20 mM MES, pH 6.0. Solid lines, experimental traces; dashed lines, simulated traces, using those values for the rate constants k_1, k_2, and k_3 in Figure 3 that give the best fit, as explained in the text. The vertical scale for the 660-nm trace is 2× enlarged. Time constant of recording, 0.25 ms.

about 20 mM in the presence of a site I anion such as nitrate.[3] The factor 0.6 accounts for the apparent difference in the quantum yields of the photoreactions of HR_{565} and $HR_{578}{\cdot}Cl^-$, as described earlier. The differential extinction coefficients were estimated to be 20 300 $M^{-1}{\cdot}cm^{-1}$ for $HR_{520}{\cdot}Cl^-$ at 500 nm and 24 500 $M^{-1}{\cdot}cm^{-1}$ for HR_{640} at 660 nm, from published spectra of halorhodopsin and $HR_{520}{\cdot}Cl^-$ (Hegemann et al., 1985), the relative absorption changes at 580 nm and 660 nm (Figure 1), and the assumption that the shape of the absorption spectrum of HR_{640} resembles that of HR_{565}. Finally, to better simulate the traces, a 0.25-ms time constant was incorporated into the calculations for the rise of the absorption changes.

The procedure of fitting the rate constants was as follows. The value of k_3 was estimated from the decay of HR_{640}, determined in the absence of chloride (as in Figure 1, trace E). The best fit (not shown) was for $k_3 = 310\ s^{-1}$. Then, traces were generated at a high chloride concentration (0.35 M), where contributions from the photoreaction of HR_{565} do not need to be considered, and k_1 and k_2 were adjusted to give the best visual fit to the experimental traces. In the comparisons, the maximum amplitude of the 500-nm simulated trace was scaled to that of the experimental trace. Agreement between simulated and experimental traces in the decay rate at 500 nm, and in the amplitude and the rise and decay rates at 660 nm, was the consequence of choosing the appropriate rate constants. A good fit could be made in this way, as shown in Figure 4. This suggested that the scheme in Figure 3 would have good predictive ability for the flash data. The values of k_1 and k_2, which generated the simulated traces in Figure 4, were 210 s^{-1} and 470 $M^{-1}{\cdot}s^{-1}$, respectively.

Next, simulated traces were obtained, by using the three rate constants so evaluated, at different chloride concentrations. Figures 5 and 6 show experimental and simulated traces at 500 and 660 nm, respectively, at selected chloride concentrations. Since at low chloride concentrations some depletion of HR_{565} will be seen at 500 nm (cf. Figure 1, trace G), the experimental 500-nm traces did not exactly correspond to the production of $HR_{520}{\cdot}Cl^-$, as originally intended. To correct

[3] B. Schobert, unpublished result.

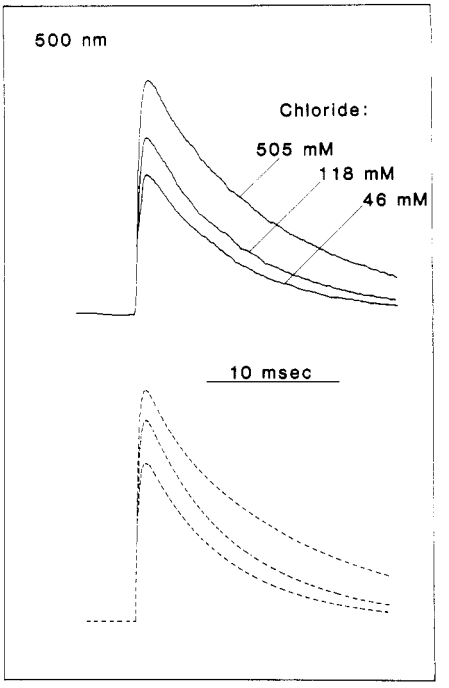

FIGURE 5: Comparison of flash-induced absorption changes at 500 nm (production of $HR_{520}{\cdot}Cl^-$) with simulated traces. The halorhodopsin (7.2 nmol/mL) was in 0.5 M Na_2SO_4 plus 100 mM $NaNO_3$ and NaCl at the indicated concentrations, and 20 mM MES, pH 6.0. Solid lines, experimental traces; dashed lines, simulated traces at the same chloride concentrations, using the same rate constants as in Figure 4. Time constant of recording, 0.25 ms.

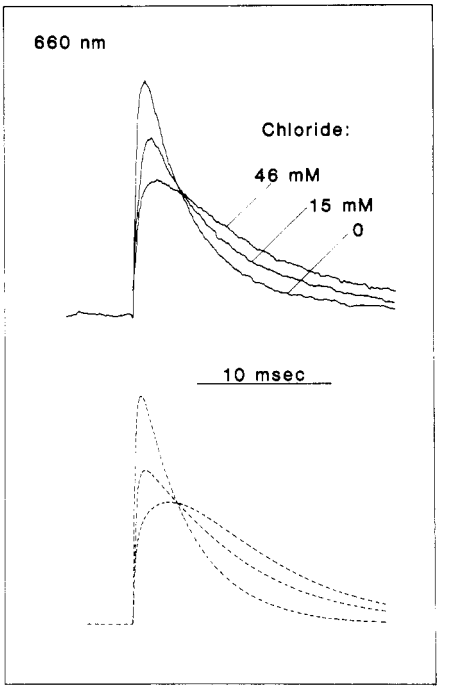

FIGURE 6: Comparison of flash-induced absorption changes at 660 nm (production of HR_{640}) with simulated traces. Experimental conditions and other details, as in Figure 5, except for the wavelength of the measurement.

for this, an appropriately scaled amount of the 660-nm trace at the same chloride concentration was added to these traces. Figures 5 and 6 shows that the simulations resemble the flash traces reasonably well, although minor differences do exist (e.g., note the simulated and experimental traces for 46 mM chloride in Figure 6). For a quantitative comparison, macroscopic kinetic parameters were determined for both simu-

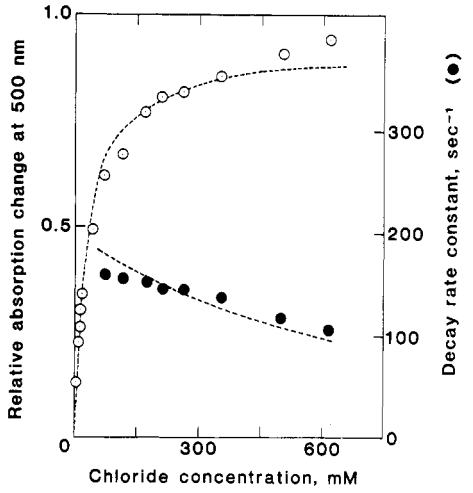

FIGURE 7: Comparison of some macroscopic kinetic parameters obtained experimentally and from the computer simulations at 500 nm (production of HR_{520}·Cl^-). Open circles, amplitudes of absorption changes after the flash, relative to that obtained at 0.35 M chloride. The maximum amplitude is set at 1 without using the instrumental time constant. Closed circles, quasi-exponential decay rate constants from the experimental traces. Dashed lines, predictions of the simulations, using the same rate constants as in Figure 4.

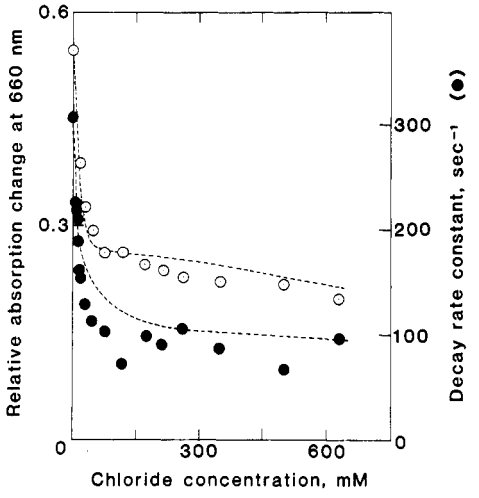

FIGURE 8: Comparison of some macroscopic kinetic parameters obtained experimentally and from computer simulations at 660 nm (production of HR_{640}). Open circles, amplitude of absorption changes after the flash, relative to that obtained at 0.35 M chloride at 500 nm. Closed circles, quasi-exponential decay rate constants from the experimental traces. Dashed lines, predictions of the stimulations, using the same rate constants as in Figure 4.

lated and experimental traces at different chloride concentrations. In Figure 7 the amplitude of the absorption change (relative to the maximal change at 500 nm) and the quasi-exponential decay rate is shown for the traces at 500 nm, with experimental points and the predicted dashed lines included. In Figure 8 the same quantities are shown for the traces at 660 nm. It is evident from these figures that the scheme in Figure 3 and the evaluated rate constants give nontrivial predictions for the parameters of the flash traces. The experimental data fit these predictions reasonably well, particularly with regard to the lack of symmetry between the chloride dependencies of the kinetics of HR_{520} and HR_{640}. The good fit indicates that pathways of conversion other than those shown in Figure 3, e.g., direct decay of HR_{520}·Cl^- into HR_{578}·Cl^-, do not contribute significantly. Nor does it seem likely that a model with two noninteracting photocycles would be valid. Although HR_{640} produced from HR_{520}·Cl^- and HR_{640} produced from HR_{565} behave identically from a kinetic point of view, validating the scheme in Figure 3 where they are designated as a single species, it is possible that they might not be identical in other kinds of measurements.

Discussion

The photocycle scheme shown in Figure 3 contains three adjustable rate constants. The flash-dependent absorption change traces at high chloride concentrations (e.g., in Figure 4, where the photoreaction of HR_{565} needs not to be considered) provide three independent kinetic parameters: the amplitude of absorption change at 660 nm relative to that at 500 nm and the macroscopic decay rates at 500 and 660 nm. The system is therefore fully determined, and fitting the model should yield unique values for each rate constant. The values obtained were $k_1 = 210\ s^{-1}$, $k_2 = 470\ M^{-1}{\cdot}s^{-1}$, and $k_3 = 310\ s^{-1}$. These rate constants were tested at various chloride concentrations by using a dissociation constant for HR_{578}·Cl^- available from independent experiments, and they were found to predict the experimental traces quite well. The scheme in Figure 3 is, therefore, a good approximation of the kinetics of the flash-induced photoreactions of halorhodopsin.

The photocycle scheme in Figure 3 includes two chloride-dependent equilibria: between the parent species, HR_{565} and HR_{578}·Cl^-, and between the photointermediates, HR_{640} and HR_{520}·Cl^-. The dissociation constant that describes the first of these equilibria is given as 0.020 M from independent measurements under the conditions of the experiments in this report. The chloride binding site in this equilibrium is that described (Schobert et al., 1986) as site II. The dissociation constant for the second equilibrium is given by k_1/k_2, which equals 0.45 M. It appears, therefore, that chloride is bound with high affinity to the parent halorhodopsin, but with much lower affinity to its photointermediate. Thus, chloride is bound, released, and then rebound during the photocycle. Release of the chloride from HR_{520}·Cl^- is possible even at physiological Cl^- concentrations (which greatly exceed 0.45 M), because of the proposed irreversible, chloride-independent conversion of HR_{640} into HR_{565} in Figure 3.

Significantly, while the parent species contain *all-trans*-retinal (Smith et al., 1984; Alshuth et al., 1985; Maeda et al., 1985), we find that the photointermediates contain *cis*-(probably 13-*cis*-) retinal (Lanyi, 1984b; this study). It is tempting to suggest therefore that it is the retinal isomerization which alters the affinity to chloride. Since anion binding to site II causes a red shift in the chromophore absorption band (Ogurusu et al., 1982; Steiner et al., 1984; Schobert et al., 1986), the interaction of chloride bound to this site with the retinal seems feasible. Interestingly, chloride binding to HR_{640} causes a large blue shift instead of the small red shift observed with HR_{565}, suggesting a different kind of interaction between the retinal and protein (and chloride) in the photointermediate.

We are currently engaged in testing the photocycle scheme with halorhodopsin-containing cell envelope vesicles, prepared from *H. halobium*. Earlier results have suggested (Schobert et al., 1983; Bogomolni et al., 1984) that the HR_{565} to HR_{578}·Cl^- equilibrium (i.e., site II) is affected by chloride on the side of the membrane from which chloride is translocated. Since these vesicles have good inside-in orientation (Lanyi & MacDonald, 1979), it should be possible to test if the equilibrium between HR_{640} and HR_{520}·Cl^- is influenced by chloride on the opposite side. If this is the case, the photocycle scheme in Figure 3 immediately suggests a transport scheme, in which the chloride ion bound to site II is translocated from a high-affinity site on one membrane surface to a low-affinity site on the other membrane surface and released there.

ACKNOWLEDGMENTS

We are grateful to Drs. G. Groma and Zs. Dancshazy for suggesting the use of photodiodes in order to improve the performance of the flash photometer. We thank Drs. D. Oesterhelt and J. Tittor for making available to us their model for the halorhodopsin photocycle before its publication and for sharing their ideas with us in many lengthy and stimulating discussions in which we came to a qualitative, if not fully quantitative, agreement over the kinetic parameters of the model.

Registry No. Cl^-, 16887-00-6.

REFERENCES

Alshuth, T., Stockburger, M., Hegemann, P., & Oesterhelt, D. (1985) *FEBS Lett. 179*, 55–59.

Bamberg, E., Hegemann, P., & Oesterhelt, D. (1984) *Biochim. Biophys. Acta 773*, 53–60.

Bogomolni, R. A., Taylor, M. E., & Stoeckenius, W. (1984) *Proc. Natl. Acad. Sci. U.S.A. 81*, 5408–5411.

Hazemoto, N., Kamo, N., Kobatake, Y., Tsuda, M., & Terayama, Y. (1984) *Biophys. J. 45*, 1073–1077.

Hegemann, P. (1984) Ph.D. Dissertation, Ludwig-Maximilian University, Munich.

Hegemann, P., Oesterhelt, D., & Steiner, M. (1985) *EMBO J. 4*, 2347–2350.

Hess, B., & Kuschmitz, D. (1979) *FEBS Lett. 100*, 334–340.

Honig, B., Dinur, U., Nakanishi, K., Balogh-Nair, V., Gawinowitz, M. A., Arnaboldi, M., & Motto, M. (1979) *J. Am. Chem. Soc. 101*, 7084–7086.

Kakitani, H., Kakitani, T., Rodman, H., & Honig, B. (1985) *Photochem. Photobiol. 41*, 471–479.

Lanyi, J. K. (1984a) *Compr. Biochem.: Bioenerg. 9*, 315–350.

Lanyi, J. K. (1984b) *FEBS Lett. 175*, 337–342.

Lanyi, J. K. (1986) *Annu. Rev. Biophys. Biophys. Chem. 15*, 11–28.

Lanyi, J. K., & MacDonald, R. E. (1979) *Methods Enzymol. 56*, 398–407.

Lanyi, J. K., & Schobert, B. (1983) *Biochemistry 22*, 2763–2769.

Maeda, A., Ogurusu, T., Yoshizawa, T., & Kitagawa, T. (1985) *Biochemistry 24*, 2517–2521.

Oesterhelt, D., Hegemann, P., & Tittor, J. (1985) *EMBO J. 4*, 2351–2356.

Ogurusu, T., Maeda, A., Sasaki, N., & Yoshizawa, T. (1981) *J. Biochem. (Tokyo) 90*, 1267–1273.

Ogurusu, T., Maeda, A., Sasaki, N., & Yoshizawa, T. (1982) *Biochim. Biophys. Acta 682*, 446–451.

Schobert, B., & Lanyi, J. K. (1982) *J. Biol. Chem. 257*, 10306–10313.

Schobert, B., Lanyi, J. K., & Cragoe, E. J., Jr. (1983) *J. Biol. Chem. 258*, 15158–15164.

Schobert, B., Lanyi, J. K., & Oesterhelt, D. (1986) *J. Biol. Chem.* (in press).

Smith, S. O., Marvin, M. J., Bogomolni, R. A., & Mathies, R. A. (1984) *J. Biol. Chem. 259*, 12326–12329.

Steiner, M., & Oesterhelt, D. (1983) *EMBO J. 2*, 1379–1385.

Steiner, M., Oesterhelt, D., Ariki, M., & Lanyi, J. K. (1984) *J. Biol. Chem. 259*, 2179–2184.

Stoeckenius, W., & Bogomolni, R. A. (1982) *Annu. Rev. Biochem. 52*, 587–616.

Tsuda, M., Hazemoto, N., Kondo, M., Kobatake, Y., & Terayama, Y. (1982) *Biochem. Biophys. Res. Commun. 108*, 970–976.

Warshel, A. (1979) *Photochem. Photobiol. 30*, 285–290.

CORRECTION

Inhibition of Enzymic Incision of Thymine Dimers by Covalently Bound 2-[*N*-[(Deoxyguanosin-8-yl)acetyl]amino]-fluorene in Deoxyribonucleic Acid, by Nahum J. Duker* and George W. Merkel, Volume 24, Number 2, January 15, 1985, pages 408–412.

Page 412. In column 1, the first sentence should read as follows: Therefore, an extraneous type of damage can reduce repair of pyrimidine dimers even though it is excised by a completely different pathway.